coatings

MDPI

Article

Nanostructured Silicon Derived from an Agricultural Residue Bagasse Ash via Magnesiothermic Reduction Method

Ntalane S. Seroka [1,*], Raymond Taziwa [2] and Lindiwe Khotseng [1,*]

[1] Department of Chemistry, University of the Western Cape, Robert Sobukwe Road, Private Bag X17, Bellville 7535, South Africa
[2] Department of Applied Science, Faculty of Science, Engineering and Technology, Walter Sisulu University, Old King William Town Road, Potsdam Site, East London 5200, South Africa
* Correspondence: 3754640@myuwc.ac.za (N.S.S.); lkhotseng@uwc.ac.za (L.K.)

Abstract: This study presents the magnesiothermic reduction of silica into silicon. This reduction process occurs at a lower reaction temperature than its carbothermal counterpart. Furthermore, silica was extracted from sugarcane bagasse ash via a thermo-chemical treatment method using, for the first time, L-cysteine chloride monohydrate and used as a precursor in the production of silicon using magnesiothermic reduction. The as-synthesized nanocrystalline silicon's physicochemical properties were investigated using XRD, Raman, FTIR, BET, and SEM. A peak at 2 of 28.2 with a crystallite size of 32 nm was discovered using X-ray diffraction spectroscopy. The pronounced peak around 518 cm^{-1} was observed from the Raman spectrum, characteristic of crystalline silicon. The FTIR analysis showed two sharp peaks at 446 cm^{-1} and 1056 cm^{-1}, indicative of the Si-O rocking mode and Si-O-Si stretching mode functional groups present. N_2 physisorption at 77 K reveals that the surface area, pore volume, and pore diameter of the as-synthesized silicon were 73 m^2/g, 0.23 cm^3/g, and 12 nm, respectively. In this study, we were able to produce silicon from silica extracted from SCBA using the magnesiothermic reduction method in a tube furnace, which has potential for thin-film solar cells.

Keywords: sugarcane bagasse ash; silica; magnesiothermic reduction; silicon; solar cell

Citation: Seroka, N.S.; Taziwa, R.; Khotseng, L. Nanostructured Silicon Derived from an Agricultural Residue Bagasse Ash via Magnesiothermic Reduction Method. *Coatings* **2023**, *13*, 221. https://doi.org/10.3390/coatings13020221

Academic Editors: Mehmet Yilmaz and Nagabandi Jayababu

Received: 15 December 2022
Revised: 12 January 2023
Accepted: 14 January 2023
Published: 17 January 2023

1. Introduction

Sugarcane bagasse ash, a waste product from the sugarcane industry, was processed into silica (SiO_2) powder in this study. An ideal process for sustainability is the production of manufactured silica particles from low-cost renewable or waste resources. Sugarcane bagasse has emerged as a sustainable resource for both tailored silica particles and bioenergy production. Furthermore, the manufacture of engineered silica particles from sugarcane bagasse ash to produce nanosilicon. Silica is a significant raw material for industrial applications, and much research has been conducted to extract it from agricultural wastes such as sugarcane bagasse, rice husk, etc. [1,2].

Silicon is an inorganic material of great technological importance across many fields owing to its inherent set of physical, chemical, electronic, and optical properties [1–3]. Due to its application-specific and superior properties, the performance profile with its synergistic high surface area and small particle size makes it a good candidate for applications in a range of new technological advances, including functional nanomaterials, biotechnology, nanoelectronics, energy production, and storage devices. Another interesting feature is the application of silicon in thermoelectric materials via magnesium alloy technology [4,5].

Presently, the crystalline silicon used in solar cell production is produced from the traditional quartz source of silica. The synthetic route is high energy intensive (around 1900 °C), which minimizes all process steps at a high operating cost, resulting in the production of highly expensive solar cells. Several studies report alternative methods

with low operating costs, including the metallothermic method, which has gained great attention as a straightforward synthesis of porous Si [6,7].

A metal, such as magnesium, zinc, or aluminum, to name a few, is used in the reduction procedure. Furthermore, the ideal metal for a reduction reaction should be cheap, easy to work with, produce eco-friendly products with a low melting point, and, most importantly, have significant redox properties. Metal oxides may be produced as by-products of these processes, which is undesirable. Nonetheless, metal oxide removal can be hazardous due to a violent reaction with water [8]. Indeed, Zn readily reacts with Si halides; however, the reaction with silica is thermodynamically unfavourable. As a result, Mg and Al are the most commonly-used metallothermic reduction agents for silica. The magnesiothermic reduction has demonstrated the ability to produce silicon from silica in the laboratory. In the temperature range between 500 and 950 °C, the magnesiothermic reduction has demonstrated the ability to synthesize silicon from silica, enabling the template-assisted creation of silicon structures [8,9].

Among the many different natural resources at our disposal, sugarcane is one of the main potential sources for silica extraction and subsequent transformation to nanostructured silicon, as tabulated in Table 1. This feedstock is traditionally used for sugar and ethanol, and the residue from the process (bagasse) is utilized as the main source of energy. In this study, experiments were carried out to convert silica nanoparticles to nanosilicon using magnesiothermic reduction. Consequently, the as-produced nanopowders were analyzed and compared in terms of physical, chemical composition, morphology, and structural properties [10].

Table 1. Recent studies reporting the magnesiothermic reduction with their results.

Precursor	Reaction Conditions	Properties of As-Produced Silicon
Algae	T = 650 °C	Nanocrystal silicon SSA-500 m^2/g, Pore Size Diameter-2 nm. [11]
SiO_2 (Stober Method)	T = 800 °C t = 12 h Argon atm	Porous nanocrystalline Si [12]
Rice Husk (RH), Bamboo Culm (BC), and Sugarcane Bagasse (SCB)	T = 650 °C t = 30 min (MW-MR)	Porous Silicon, Pore diameter (50–80 nm) SSA [13]
RH	T = 650 °C t = 7 h	Porous silicon SSA 150 m^2/g [14]

2. Experimental

2.1. Materials Used

All chemicals were purchased from Sigma-Aldrich and used without further purification. L-cysteine hydrochloride monohydrate (98%) and tetrapropylammonium hydroxide (1.0 M) in H_2O were purchased from Sigma-Aldrich (St. Louis, MO, USA). Sugarcane was procured from the Sugar Illovo South Africa Company (KwaZulu-Natal, South Africa). In a typical preparation procedure, sugarcane bagasse was soaked for a period of 24 h in double-deionized water to remove any dust and soil particles. The soaked sugarcane was then oven-dried for a period of 6 h. After being soaked and dried, the sugarcane was burned in the open air to produce black sugarcane bagasse ash (SCBA). The synthesis was done using deionized water from the Milli-Q water purification system (Millipore, Bedford, MA, USA).

The chemical composition test was done using X-ray fluorescence spectroscopy (XRF, (Malvern Panalytical, Malvern, UK) for major oxides present in the SCBA in Table 2. The XRF study reveal that the leaching process was efficient as the amount of silica was significantly reported to be 79.40 wt%. The pretreatment step was done using L-cysteine hydrochloride monohydrate as the leaching acid. The loss on ignition is also reported in Table 2.

Table 2. Chemical composition of acid-leached SCBA from XRF.

Component	Wt%
SiO_2	79.40
TiO_2	1.03
Al_2O_3	8.45
Fe_2O_3	2.39
MnO	0.04
MgO	0.61
CaO	1.06
Na_2O	1.06
K_2O	3.86
P_2O_5	0.22
SO_3	0.03
Cr_2O_3	0.04
NiO	0.02
H_2O	0.04
LOI	1.18

The significant improvement in the morphology of silica in the powders of the ash is due to the selective removal of the synthesis residues using L-cysteine hydrochloride monohydrate, essentially reducing metallic impurities in the sample. After acid-treatment, the sample was calcined in a muffle furnace and subsequent extraction of silica via hydrothermal method using tetrapropylammonium hydroxide, thereby minimizing the other metal oxides impurities.

2.2. Magnesiothermic Reduction of Silica to Silicon

The as-synthesized biosilica from sugarcane bagasse ash and Mg chips used for the magnesiothermic reduction were 2.5 g and 3.0 g, respectively, as shown in reaction 1. The mixture was subjected to pyrolysis at 700 °C for 4 h in a tube furnace under nitrogen (at 10 °C/min heating rate). A portion of dark brownish and greyish powder (as-reduced silica) was immersed in HCl solution, shown in reaction 2, and reflux at 100 °C for 2 h to remove excess Mg and unreacted silica, using a modified method reported in previous studies by Bao Z, et al., 2007 [13].

$$SiO_2 + 2Mg \rightarrow Si + 2MgO \quad (1)$$

$$Si + MgO + HCl \rightarrow Si(s) \downarrow + MgCl_2(aq) \quad (2)$$

The resulting gray solution was then filtered using a Buchner funnel. The trapped precipitate was then washed with double-deionized water and decanted until the pH of the supernatant reached 6.5. The resulting gray precipitate was then dried in an oven at 40 °C overnight and ground into a fine powder. Subsequently, nanosilicon was produced. The actual dark grey powder silicon was further studied for physico-chemical properties using Raman spectroscopy (Hamamatsu photonics, Japan) for purity, Fourier Transform Infrared spectroscopy (Perkin Elmer, Waltham, MA, USA) for evolution of surface chemistry, Brunauer-Emmett-Teller (BET, Thermofischer Scientific, Waltham, MA, USA) for textural properties (specific surface area, pore volume, and pore diameter), and morphological studies were done using a scanning electron microscope (SEM-EDX), (TESCAN, VEGA, JEOL, Peabody, MA, USA) coupled with EDX (energy X-ray dispersive spectroscopy).

3. Results and Discussion

3.1. X-ray Diffraction (XRD) and Raman Spectroscopy

The XRD and Raman analyses were performed on the material prepared by magnesiothermic reduction to study the crystallinity and vibration as well as structural properties, respectively. The phase identification from XRD analysis was cross-examined on SCBA nano-Si, whose 2θ angle of 28.2 (Figure 1a) showed peaks of highly crystalline silicon, which can be compared with the JCPDS (No. 27–1402 Si XRD) reference pattern number. The crystallite size estimated by the Scherrer equation based on the peak (inset) at 2θ of 28.2 was 32 nm.

Scherrer equation: $\mathrm{Dp} = \frac{K\lambda}{\beta \cos\theta}$, whereby Dp-Average crystallite size (nm), K-Scherrer constant. It varies from 0.68 to 2.08 and K = 0.94 for spherical crystallites with cubic symmetry, λ-X-ray wavelength. For mini XRD, $CuK\alpha$ average = 1.54178 A, B-FWHM (full Width at Half Maximum) of XRD peak, θ-XRD peak position, one half of 2θ.

Despite the fact that the as-synthesized silicon has a well-defined crystalline structure, the presence of a small halo centered at $2\theta = 22.5$, characteristic of an amorphous property in the material, is quite interesting; similar results have been reported by [15,16].

This confirms the successful reduction of silica into nano-silicon from sugarcane bagasse ash. The structural properties were carried out using Raman spectroscopy for the as-synthesized SCBA nano-silicon, as presented in Figure 1b. The Raman spectra with a peak at 518 cm^{-1}, characteristic of Si-Si stretching mode, shown in the inset, and the half-full width at half maximum (FWHM) of 6 cm^{-1} were observed; similar results were reported by Li et al. This was as a result of the scattering of the first-order optical phonon of nanosilicon. In their study of the Raman spectrum for crystalline silicon, they observed a peak at 520 cm^{-1} and a FWHM of 2.8 cm^{-1} [17,18].

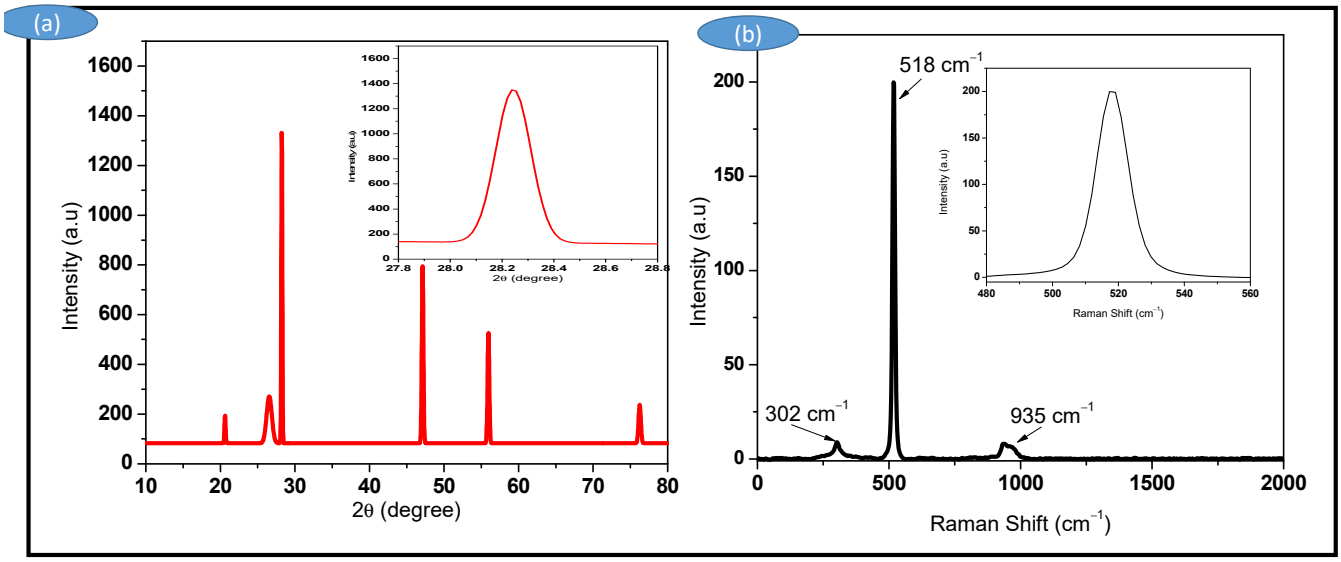

Figure 1. XRD pattern (**a**) and Raman spectrum (**b**) of SCBA nano silicon prepared by magnesiothermic reaction.

The other two peaks observed at 302 cm^{-1} and 935 cm^{-1}, respectively, were emanating from the scattering of two transverse acoustic (2TA) phonons and two optical (2TO) phonons, respectively. The peak at 935 cm^{-1} is reported in the literature due to the stretching mode of amorphous Si-Si. Interestingly, Li et al. [9] reported 300 cm^{-1} and 970 cm^{-1} as the observations for 2TA and 2TO, respectively [17,18].

As a result, Holzapfel et al. [19] reported a significant feature of silicon signals with the most desirable Raman characteristic at 518 cm^{-1} and a full width at half maximum (FWHM) of 6 cm^{-1}, similar to the current study's results. As a result, the scattering of first-order optical phonon mode (TO) was assigned. The two peaks at 300 cm^{-1}, and

900 cm^{-1} were notably assigned to the scattering of the second-order transverse acoustic phonon mode (2TA) and the second-order optical phonon mode (2TO), respectively [17–19].

3.2. FTIR Spectroscopy

The evolution of the FT-IR spectra of nanosilicon prepared from the magnesiothermic reduction of silica extracted from sugarcane bagasse ash is presented in Figure 2, and the characteristic bond peaks that appeared in the spectra are tabulated in Table 3.

Table 3. Typical bond peaks appearing in FTIR spectra for SCBA nano-Si.

Wavelength (cm^{-1})	Bond	Type
1056	Si-O	Stretching mode
446	Si-O	Rocking vibration

The Si-O stretching mode (1056 cm^{-1}) and Si-O rocking vibration (446 cm^{-1}) are observed in the powder samples. A major contribution to the increase of the Si-O bond comes from the aging of the Si nanoparticles. It is highly probable that these bonds are formed by the combination of O_2 present in the DI water; a similar conclusion was made in the literature [20,21].

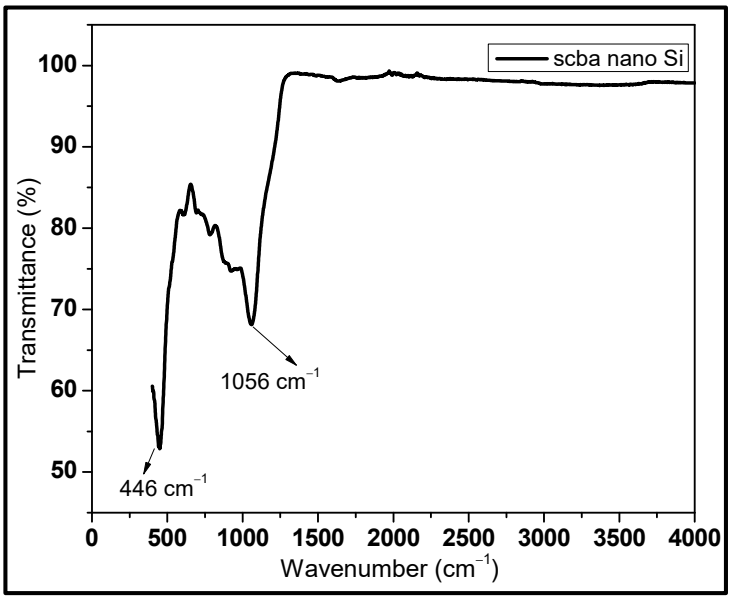

Figure 2. FTIR spectrum showing surface chemistry of SCBA nano silicon.

3.3. Nitrogen Physisorption Studies

The interfacial properties of the as-synthesized SCBA nanosilicon were studied via the N_2 adsorption–desorption method, and the results are reported in Table 4 below.

Table 4. Textural properties of sugarcane bagasse ash nano silicon.

Sample ID	BET_{SSA} (m^2/g)	Vp (cm^3)	Dp (nm)
SCBA nano-silicon	74	0.23	12

The values for the specific surface area obtained by the BET analysis were 74 m^2/g, a pore volume of 0.23 cm^3, and a pore diameter of 12 nm for the SCBA nanosilicon. When the hysteresis loop was present at a range of $0.6 < P/P_0 < 1.0$ from the graph, the degree of porosity was observed. And the loop is associated with large pores [22].

It is interesting to note that the material prepared via the thermo-chemical treatment method was observed to have a moderate increase in specific surface area, porosity, pore volume, and average pore diameter in relation to the increasing P/P_0 at the lower P/P_0 regions, as shown in Figure 3. Moreover, the adsorption isotherm of the as-prepared SCBA nanosilicon had similar features as those presented in [22–24].

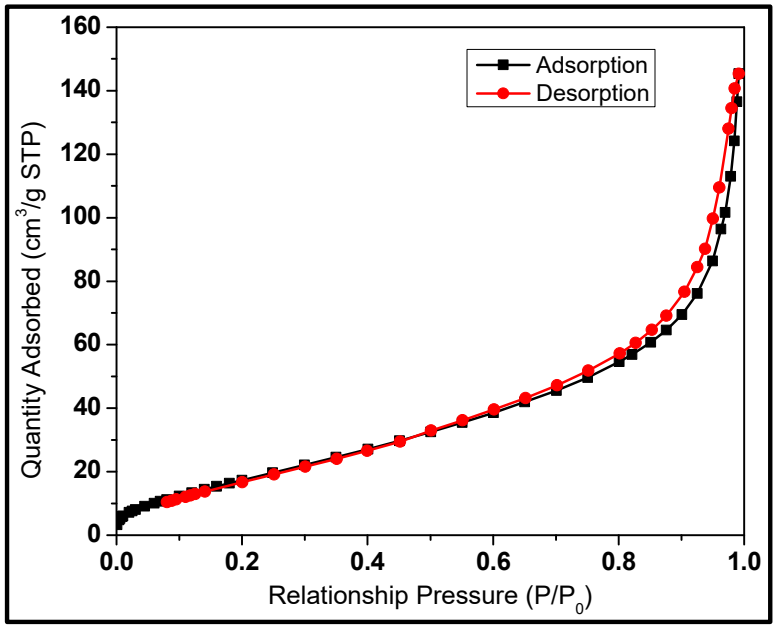

Figure 3. N_2 adsorption-desorption isotherm for the powder SCBA nano silicon prepared by thermo-chemical method.

3.4. Scanning Electron Microscopy (SEM) Analysis

The SEM images are presented in Figure 4a,b at different magnifications. At higher magnifications, agglomerates of SCBA nanosilicon of irregular shapes can be seen, as well as the presence of some spherical particles distributed in a porous structure. This transformation is as a result of the particles having sizes in the nanometric scale consistent with the XRD results, the grain size was in the range 30 nm to 500 nm [24].

The surface morphologies of nano-silicon produced show nanoparticle agglomeration, which is favoured by the magnesiothermic reduction step. As shown in Figure 4c, the process efficacy was assessed using energy dispersive X-ray spectroscopy (EDX). The strong intensity of oxygen and silicon shown in the EDX spectra confirms the silica element is present in the sample. This is a negligible impurity commonly associated with the green method. This may be due to the resultant surface of highly active silicon upon exposure to the aqueous solution of HCl as well as the small presence of unreacted silica in the sample during the reduction method [24,25]. The morphological changes are in agreement with the surface chemistry discussed earlier in the FTIR analysis.

The SEM-EDX analysis presented in Figure 4c confirms that magnesiothermic reduction of silica into silicon is an effective tool in harnessing sugarcane bagasse ash for valuable materials such as silicon nanoparticles. The predominantly as-synthesized silicon content in the sample is indicative that the agro-waste SCBA is rich, useful, and cost-effective for the synthesis of silicon.

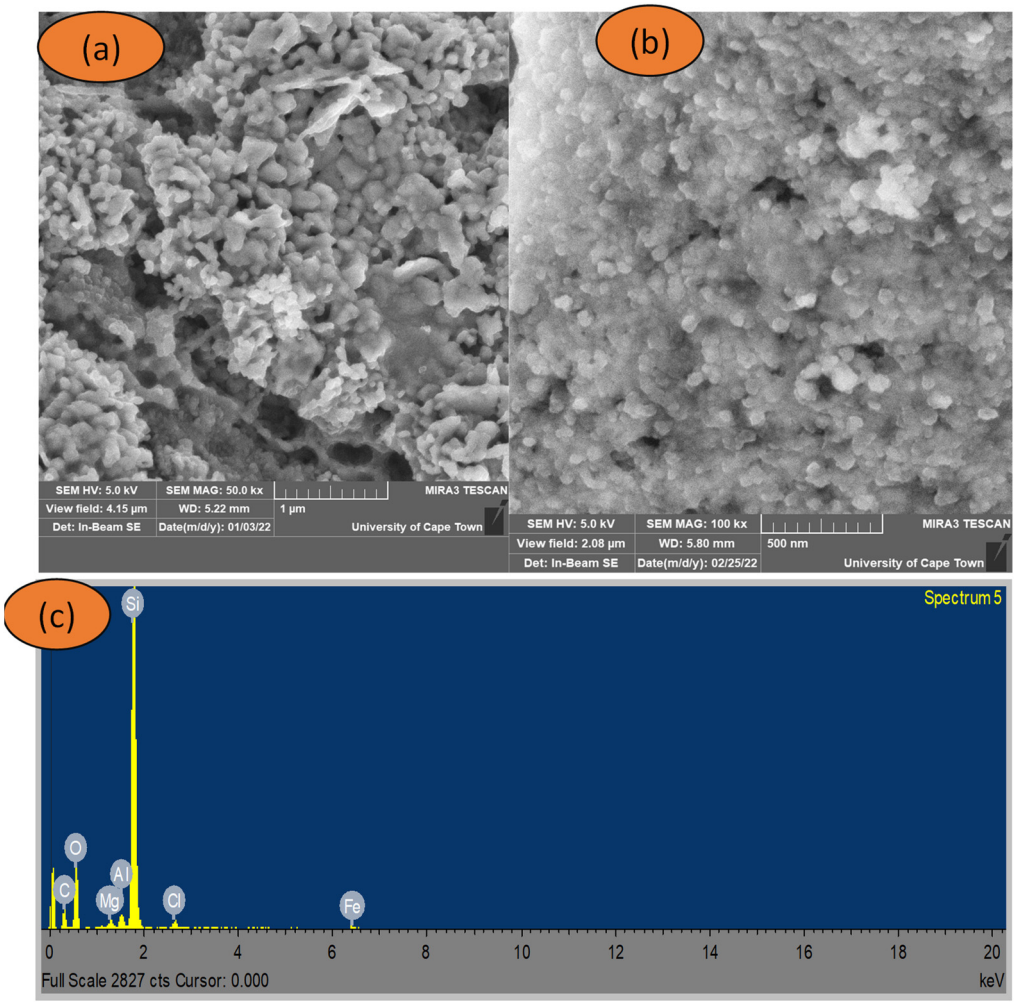

Figure 4. SEM images of (**a**,**b**) SCBA nano silicon and EDX spectrum (**c**) of SCBA nano silicon.

4. Conclusions

Based on the findings, silica extracted from sugarcane bagasse ash by L-cysteine chlorination-hydrothermal treatment was used as a precursor for the preparation of nano silicon by magnesium thermal reduction method. The nanosilicon nanoparticles were successfully synthesized from extracted biosilica from sugarcane bagasse ash (SCBA). The physical characteristics and quantitative elemental composition of nano-silicon were investigated. The surface area, pore volume, and pore diameter of the as-synthesized silicon were 74 m^2/g, 0.23 cm^{-1}, and 12 nm, respectively. According to Raman spectroscopy, a frequency downshift is caused by a decrease in particle size as a result of particle surface oxidation. The FTIR spectrum confirms the increase in oxidation of the particles during washing with deionized water, with peaks at 446 cm^{-1} and 1056 cm^{-1}, respectively, corresponding to rocking and stretching modes. The morphological, textural, and structural properties determined in this study indicated that the as-produced material exhibits highly rich silicon with a well-defined crystalline structure with a diameter of 32 nm. Moreover, these results showed that nanostructured silicon can be produced from sustainable sources of silica. Magnesiothermic process serves as a potential method for the production of silicon due to its low operating costs, and due to its high violent reactivity, sodium chloride is often used as a stabilizer for an efficient and stable process, and can rival a conventional carbothermal process.

Author Contributions: Conceptualization, N.S.S. and R.T.; methodology, N.S.S.; software, N.S.S.; validation, N.S.S., R.T. and L.K.; formal analysis, N.S.S.; investigation, N.S.S.; resources, L.K.; data curation, N.S.S.; writing—original draft preparation, N.S.S.; writing—review and editing, L.K.; visualization, N.S.S.; supervision, R.T. and L.K.; project administration, L.K.; funding acquisition, L.K. All authors have read and agreed to the published version of the manuscript.

Funding: This research was funded by National Research Foundation: 138079 and Eskom (South Africa): 2002/015527/0.

Institutional Review Board Statement: Not applicable.

Informed Consent Statement: Not applicable.

Data Availability Statement: All data that support the findings of this study are included within the article.

Conflicts of Interest: The Authors declare no conflict of interest.

References

1. Yadav, M.; Dwibedi, V.; Sharma, S.; George, N. Biogenic silica nanoparticles from agro-waste: Properties, mechanism of extraction and applications in environmental sustainability. *J. Environ. Chem. Eng.* **2022**, *10*, 108550. [CrossRef]
2. Praneetha, S.; Murugan, A.V. Development of sustainable rapid microwave assisted process for extracting nanoporous Si from earth abundant agricultural residues and their carbon-based nanohybrids for lithium energy storage. *ACS Sustain. Chem. Eng.* **2015**, *3*, 224–236. [CrossRef]
3. Liu, N.; Huo, K.; McDowell, M.T.; Zhao, J.; Cui, Y. Rice husks as a sustainable source of nanostructured silicon for high performance Li-ion battery anodes. *Sci. Rep.* **2013**, *3*, 1919. [CrossRef] [PubMed]
4. Guo, M.; Zou, X.; Ren, H.; Muhammad, F.; Huang, C.; Qiu, S.; Zhu, G. Fabrication of high surface area mesoporous silicon via magnesiothermic reduction for drug delivery. *Microporous Mesoporous Mater.* **2011**, *142*, 194–201. [CrossRef]
5. Jeong, J.H.; Kim, K.H.; Jung, D.W.; Kim, K.; Lee, S.M.; Oh, E.S. High-performance characteristics of silicon inverse opal synthesized by the simple magnesium reduction as anodes for lithium-ion batteries. *J. Power Sources* **2015**, *300*, 182–189. [CrossRef]
6. Zhou, Z.; Han, G.; Lu, X.; Wang, G.; Zhou, X. High-performance magnesium-based thermoelectric materials: Progress and challenges. *J. Magnes. Alloys* **2022**, *10*, 1719–1736. [CrossRef]
7. Zhong, H.; Zhan, H.; Zhou, Y.H. Synthesis of nanosized mesoporous silicon by magnesium-thermal method used as anode material for lithium ion battery. *J. Power Sources* **2014**, *262*, 10–14. [CrossRef]
8. Huang, Z.G.; Gao, K.; Wang, X.G.; Xu, C.; Song, X.M.; Shi, L.X.; Zhang, Y.; Hoex, B.; Shen, W.Z. Large-area MACE Si nano-inverted-pyramids for PERC solar cell application. *Sol. Energy* **2019**, *188*, 300–304. [CrossRef]
9. Li, M.; Dai, Y.; Ma, W.; Yang, B.; Chu, Q. Review of new technology for preparing crystalline Silicon solar cell materials by metallurgical method. *IOP Conf. Ser. Earth Environ. Sci.* **2017**, *94*, 012016. [CrossRef]
10. Inasawa, S.; Ono, Y.; Mizuguchi, T.; Sunairi, A.; Nakamura, S.I.; Tsuji, Y.; Yamaguchi, Y. Cross-sectional analysis of the core of silicon microparticles formed via zinc reduction of $SiCl_4$. *CrystEngComm* **2017**, *19*, 2681–2686. [CrossRef]
11. Shen, P.; Uesawa, N.; Inasawa, S.; Yamaguchi, Y. Characterization of flowerlike silicon particles obtained from chemical etching: Visible fluorescence and superhydrophobicity. *Langmuir* **2010**, *26*, 13522–13527. [CrossRef]
12. Bao, Z.; Weatherspoon, M.R.; Shian, S.; Cai, Y.; Graham, P.D.; Allan, S.M.; Ahmad, G.; Dickerson, M.B.; Church, B.C.; Kang, Z.; et al. Chemical reduction of three-dimensional silica micro-assemblies into microporous silicon replicas. *Nature* **2007**, *446*, 172–175. [CrossRef]
13. Kim, K.H.; Lee, D.J.; Cho, K.M.; Kim, S.J.; Park, J.K.; Jung, H.T. Complete magnesiothermic reduction reaction of vertically aligned mesoporous silica channels to form pure silicon nanoparticles. *Sci. Rep.* **2015**, *5*, 9014. [CrossRef]
14. Xing, A.; Tian, S.; Tang, H.; Losic, D.; Bao, Z. Mesoporous silicon engineered by the reduction of biosilica from rice husk as a high-performance anode for lithium-ion batteries. *RSC Adv.* **2013**, *3*, 10145–10149. [CrossRef]
15. Seroka, N.S.; Taziwa, R.; Khotseng, L. Green Synthesis of Crystalline Silica from Sugarcane Bagasse Ash: Physico-Chemical Properties. *Nanomaterials* **2022**, *12*, 2184. [CrossRef]
16. Atkins, P.; Overton, T. *Shriver and Atkins' Inorganic Chemistry*; Oxford University Press: New York, NY, USA, 2010.
17. Li, B.; Yu, D.; Zhang, S.L. Raman spectral study of silicon nanowires. *Phys. Rev. B* **1999**, *59*, 1645. [CrossRef]
18. Xia, H.; He, Y.L.; Wang, L.C.; Zhang, W.; Liu, X.N.; Zhang, X.K.; Feng, D.; Jackson, H.E. Phonon mode study of Si nanocrystals using micro-Raman spectroscopy. *J. Appl. Phys.* **1995**, *78*, 6705–6708. [CrossRef]
19. Holzapfel, M.; Buqa, H.; Hardwick, L.J.; Hahn, M.; Würsig, A.; Scheifele, W.; Novák, P.; Kötz, R.; Veit, C.; Petrat, F.M. Nano silicon for lithium-ion batteries. *Electrochim. Acta* **2006**, *52*, 973–978. [CrossRef]
20. Richter, H.; Wang, Z.P.; Ley, L. The one phonon Raman spectrum in microcrystalline silicon. *Solid State Commun.* **1981**, *39*, 625–629. [CrossRef]
21. Zhang, S.L.; Wang, X.; Ho, K.S.; Li, J.; Diao, P.; Cai, S. Raman spectra in a broad frequency region of p-type porous silicon. *J. Appl. Phys.* **1994**, *76*, 3016–3019. [CrossRef]

22. Kale, P.G.; Solanki, C.S. Synthesis of si nanoparticles from freestanding porous silicon (PS) film using ultrasonication. In Proceedings of the 2010 35th IEEE Photovoltaic Specialists Conference, Honolulu, HI, USA, 20–25 June 2010; pp. 003692–003697.
23. Lee, J.H.; Kwon, J.H.; Lee, J.W.; Lee, H.S.; Chang, J.H.; Sang, B.I. Preparation of high purity silica originated from rice husks by chemically removing metallic impurities. *J. Ind. Eng. Chem.* **2017**, *50*, 79–85. [CrossRef]
24. Gregg, S.J.; Sing, K.S.W.; Salzberg, H.W. Adsorption surface area and porosity. *J. Electrochem. Soc.* **1967**, *114*, 279Ca. [CrossRef]
25. Falk, G.; Shinhe, G.P.; Teixeira, L.B.; Moraes, E.G.; de Oliveira, A.N. Synthesis of silica nanoparticles from sugarcane bagasse ash and nano-silicon via magnesiothermic reactions. *Ceram. Int.* **2019**, *45*, 21618–21624. [CrossRef]